Journal of Computational Physics **173,** 600–619 (2001)
doi:10.1006/jcph.2001.6898, available online at http://www.idealibrary.com on IDEAL®

ν-DSMC: A Fast Simulation Method for Rarefied Flow

M. N. Macrossan

Center for Hypersonics, University of Queensland, Brisbane, Australia 4072
E-mail: M.Macrossan@mailbox.uq.edu.au

Received November 15, 2000; revised June 26, 2001

A new approximate simulation method for rarefied flows, ν-DSMC, is described and tested by comparison with results from Bird's direct simulation Monte–Carlo (DSMC) method, and with a previously proposed 'relaxation time' simulation method (RTSM) which solves the BGK equation. Both ν-DSMC and RTSM execute about twice (or more) as fast as DSMC. In ν-DSMC all collision pairs (amongst near neighbours) are equally likely so the collision loops are suitable for parallel execution. In order to reproduce *any* desired viscosity law $\mu = \mu(T)$ the collision rate must be altered by making the total collision cross-section a function of the local kinetic temperature. The approximate methods have been compared to DSMC in three test cases: (1) simple relaxation calculations, (2) high speed Couette flow, and (3) the plane normal shock problem. Both approximate methods produce the same relaxation rate as DSMC, but only the new method produces a nonequilibrium distribution function similar to that for DSMC. For the Couette flow, ν-DSMC produces profiles of flow velocity, density, and temperature which agree with DSMC results to within 3–5%, while the BGK solution produces temperatures which are up to 18% greater. Similar results were found for the normal shock wave. ν-DSMC predicts the location and size of the peak T_x temperature more accurately than does RTSM. The deviation of the temperature profiles from the DSMC results are 2–3 times greater for RTSM than for ν-DSMC. The conclusion from all test cases is clear: the incorrect Prandtl number predicted by the BGK equation detracts from the usefulness of the BGK equation as a model for rarefied flow; the new approximate simulation method is just as fast as solving the BGK equation and gives results which are in much better agreement with DSMC.

Key Words: rarefied flow; numerical simulation (65C); DSMC; collision rate method; molecular dynamics (82A71).

0021-9991/01 $35.00

1. INTRODUCTION

Bird's direct simulation Monte–Carlo (DSMC) method [3] is the standard computational method for rarefied flows, where the governing equation is the Boltzmann equation. In DSMC the flow is represented by a large number of simulator particles, and the evolution of the flow is tracked by calculating the motion of these particles and their collisions amongst themselves and with any boundaries. The simulation is advanced in time steps of duration Δt which, for accuracy, should be less than the mean time between collisions. During each time step the convection and collision calculations are decoupled. First the particles are moved in collisionless flight, according to their velocities. Next the particles are frozen in position and binary collisions are calculated for some of the particles. Although the collision partners are near neighbours, they are not necessarily within one particle diameter, and the relative orientation of the trajectories of the collision partners is ignored. Postcollision velocities are calculated for the given relative speed of collision and a randomly chosen set of impact parameters. The probability of collision for each collision pair, and the total number of collisions, reflect the theoretical probability and total collision rate for the particular collision cross-section used.

The history of the development of phenomenological collision models for DSMC suggests that not every detail of the collision processes need be modeled accurately in order to obtain useful results. Recently [10], I proposed a particle simulation method in which the relaxation time or Bhatnagar-Gross-Krook (BGK) approximation [1] to the collision term in the Boltzmann equation was used to simulate the effect of collisions, without calculating any collisions. This relaxation time simulation method (RTSM) is discussed briefly in the next section, along with similar but not identical methods proposed previously by Nanbu [13, 14] and Montanero *et al.* [11]. Although these methods are computationally efficient compared to DSMC, they suffer from the same defect as does the BGK equation itself; the Prandtl number is unity, whereas the Boltzmann equation yields $Pr = 2/3$.

The purpose of this paper is to present a new approximate simulation method for the Boltzmann equation that produces any desired viscosity law and the correct Prandtl number. The new method, which I have termed 'collision frequency DSMC' or ν-DSMC, uses the particularly simple collision dynamics of the Maxwell–VHS model (that is, a Maxwell total cross-section with hard sphere scattering) to make it computationally efficient. The collision rate of the Maxwell–VHS model must be adjusted to produce **any** desired viscosity law.

The new method has been tested and compared to both DSMC and the BGK simulation method. The test cases considered are (a) a number of zero-dimensional relaxation calculations, (b) one-dimensional high-speed Couette flow, and (c) the calculation of the internal structure of a plane normal shock. Both ν-DSMC and RTSM run at twice the speed of standard DSMC. The new method produces results within 3% of those produced by DSMC for the shock structure and within 5% for the Couette flow, for Knudsen numbers ranging from $Kn \approx 0.1$ to $Kn \approx 0.005$.

2. RELAXATION TIME METHOD

The collision term of the Boltzmann equation describes how the distribution function $f(v, t)$ for particle velocities v should change with time t during the collision phase of a simulation. According to the relaxation time (BGK) approximation the collision term can

be approximated as

$$\left[\frac{\partial nf}{\partial t}\right]_{coll} = n\nu(f_e - f) = \frac{n}{\tau}(f_e - f), \tag{1}$$

where n is the number density of molecules, ν is a characteristic frequency, and $\tau = \nu^{-1}$ is the corresponding characteristic time. The exact solution of (1) is

$$(f(t') - f_e) = (f(0) - f_e)\exp(-t'/\tau), \tag{2}$$

where f_e is the local Maxwell equilibrium distribution function and $f(0) = f(t' = 0)$ is the distribution of particle velocities established by the convection phase of the simulation, before the effect of collisions is simulated. In other words, the distribution function relaxes towards equilibrium with a time constant of τ, which is the same for all velocities. After a collision interval of $t' = \Delta t$, the distribution function according to (2) is

$$f(\Delta t) = (1 - \exp(-\Delta t/\tau))\, f_e + \exp(-\Delta t/\tau)\, f(0). \tag{3}$$

In the relaxation time simulation method (RTSM) the collision phase of DSMC is replaced by a 'redistribution phase' in which a subset of the particles in the cell, a fraction

$$1 - \exp(-\Delta t/\tau)$$

of the total, are assigned new velocities characteristic of the local Maxwell distribution for the subset [10]. The velocities of the remaining fraction of particles are unchanged. The final distribution of particle velocities is a mixture of the initial distribution in the cell and a statistical approximation of the final equilibrium distribution and is thus a statistical (rather than an exact) representation of the BGK distribution of (3). This method has many features in common with Pullin's equilibrium particle simulation method [15] in which *all* the particles in the cell were assigned new equilibrium velocities at each time step. Pullin's method is the infinite collision rate limit of Bird's DSMC, or the $\tau \to 0$ limit of the RTSM method, for a given cell structure and time step.

Nanbu [13, 14] appears to be the first to have proposed a particle simulation method for the BGK equation. A recent example is that of Montanero *et al.* [11]. Both these methods differ in some respects from RTSM. In each, new equilibrium velocities are assigned to a fraction

$$\nu\Delta t = \Delta t/\tau$$

of the particles in the cell, rather than the fraction

$$1 - \exp(-\Delta t/\tau) = \Delta t/\tau - (\Delta t/\tau)^2/2! + (\Delta t/\tau)^3/3! - \cdots$$

Thus, these methods simulate a collision process (occurring at the collision rate ν) in which the postcollision velocities conform to the local equilibrium distribution; complete equilibrium is established after one collision/particle ($\Delta t = \tau$), whereas the BGK equation indicates that an infinite number of collisions/particle is required to establish equilibrium.

In addition, both the earlier methods differ slightly from RTSM in that the new velocities are selected from an equilibrium distribution that has a mean and variance matching those

of the entire set of cell velocities at the beginning of the relaxation phase, rather than the subset which undergoes a relaxation. At first glance the earlier methods would appear to be superior in that a larger sample is used to estimate the local equilibrium state, but this is not entirely clear, because in both methods, after the new velocities are selected, the total momentum and energy in the cell is not conserved. This nonconservation is accepted as part of Nanbu's method, but it is worth noting that it was a similar nonconservation effect in Nanbu's simulation method for the Boltzmann equation [12], which appears to produce greater scatter in the results compared to DSMC, that led to the general abandonment of Nanbu's method.

In Montanero's method [11], the velocities after the relaxation are 'adjusted' in order to preserve total momentum and energy in the cell. It is not clear whether this adjustment is confined to the new velocities, in which case the method is identical in this respect to RTSM, or whether all the velocities in the cell are adjusted. If the latter, it is then not clear that the final velocities after adjustment are a better representation of a mixture of the initial and equilibrium distributions than the final velocities for RTSM.

The Chapman–Enskog viscosity [6] for the relaxation time approximation is $\mu = \rho RT\tau$, from which

$$\tau = \frac{\mu}{\rho RT} = \frac{\mu}{nkT}, \tag{4}$$

where $R = k/m$ is the ordinary gas constant, k is Boltzmann's constant, m is the mass of one molecule, n is the number density, and ρ is the mass density. The appropriate value of the relaxation time τ in any cell can be determined from *any* desired viscosity for the local conditions in the cell. Thus

$$\tau = \frac{\mu(T_{kin})}{\rho RT_{kin}}, \tag{5}$$

where T_{kin} is the local kinetic temperature derived from the total thermal energy in any cell.

This relaxation time is slightly larger than the nominal collision time often derived (*via* the nominal mean free path) from viscosity. Thus

$$\lambda_{nom} = 2\mu/(\rho\bar{c}) \tag{6}$$

and

$$\tau_{nom} = \lambda/\bar{c} = (\pi/4)\mu/(\rho RT), \tag{7}$$

where

$$\bar{c} = (8RT/\pi)^{\frac{1}{2}} \tag{8}$$

is the mean thermal speed at equilibrium.

3. VHS

The most common collision model now used in DSMC calculations is the variable hard sphere model; the total collision cross-section varies with relative velocity in the same

manner as for molecules with an inverse power repulsive potential, but the scattering is as for hard spheres—all directions of the postcollision relative velocity are equally likely. The first DSMC application of this combination of hard sphere scattering and a variable total cross-section can be found in the papers of Borgnakke and Larsen [4, 5, 8], and later papers by Erofeev and Perepukhov [7] and Bird [2]. The total cross-section σ for the VHS model, as a function of relative collision speed g, is

$$\sigma(g) = \sigma_r (g_r/g)^{2\upsilon}, \tag{9}$$

where g_r and σ_r are reference values of the collision speed and total cross-section, respectively, and υ is a constant.

The Chapman–Enskog viscosity, with this total cross-section and isotropic scattering is [3]

$$\mu = \frac{15}{8\Upsilon_4} \frac{(mkT)^{\frac{1}{2}} (4RT)^{\upsilon}}{\sigma_r g_r^{2\upsilon}}, \tag{10}$$

where, for later reference, the notation

$$\Upsilon_j = \Gamma(j - \upsilon)/\pi^{\frac{1}{2}} \tag{11}$$

has been used, where Γ is the Gamma function. In other words, the viscosity is $\mu = \mu_{ref}(T/T_{ref})^{\omega}$, where

$$\omega = \frac{1}{2} + \upsilon. \tag{12}$$

3.1. Collision Frequency for VHS

The collision frequency for a total cross-section $\sigma = \sigma(g)$ is given by

$$\nu_c = n\langle g\sigma \rangle,$$

where $\langle g\sigma \rangle$ denotes the average taken over all collisions. For the VHS cross-section (9) we have

$$\nu_{VHS} = n\sigma_r g_r^{2\upsilon} \langle g^{1-2\upsilon} \rangle. \tag{13}$$

Bird [3] gives the distribution of g for equilibrium conditions, and with $g_r = (4RT_e)^{\frac{1}{2}}$, the equilibrium collision rate can be evaluated as

$$\nu_{VHS} = 2\Upsilon_2 n (4RT)^{\frac{1}{2}} \sigma_r. \tag{14}$$

From (10), also with $g_r = (4RT)^{\frac{1}{2}}$, we have

$$\sigma_r = \frac{15}{8\Upsilon_4} \frac{(mkT)^{\frac{1}{2}}}{\mu} \tag{15}$$

so that (14) becomes

$$\nu_{VHS} = \frac{15\Upsilon_2}{2\Upsilon_4} \frac{\rho RT}{\mu}. \tag{16}$$

The probability of collision for each collision pair must be proportional to the collision volume

$$g\sigma(g)\Delta t$$

so pairs of particles are accepted or rejected for collision based on this probability. This is particularly time consuming—not only must many collision pairs be sampled before one is accepted, but the collision loop is not suitable for parallel computation.

A special case is the 'Maxwell VHS' collision model, for which $\upsilon = 1/2$ in (9), and the total collision cross-section is

$$\sigma = g_r\sigma_r/g.$$

In this case all collision pairs in a cell are equally likely, so collisions can be calculated without sampling the distribution of relative velocities. The Maxwell total cross-section, with hard sphere scattering, forms the basis of the new method proposed here. From (16), with $\upsilon = \frac{1}{2}$, the collision frequency for Maxwell–VHS scattering is

$$\nu = 2\frac{\rho RT}{\mu}. \tag{17}$$

4. THE PROPOSED ν METHOD

In its basic form, the Maxwell–VHS collision model will produce a viscosity which varies linearly with temperature (see (10) with $\upsilon = 1/2$), but by making the reference cross-section σ_r a function of kinetic temperature the Maxwell–VHS model can produce any variation of viscosity with temperature, at least for near equilibrium conditions. The theoretical value of the Prandtl number is $Pr = 2/3$, as for any VHS collision model.

This modified-VHS method, which I have called 'collision rate DSMC' or ν-DSMC, can best be described with the following algorithm for its implementation (some further programming details are addressed in the Appendix):

- At each time step, calculate the kinetic temperature T_{kin} in each cell.
- Use (17) to calculate the mean collision frequency as

$$\nu_c = 2\frac{nkT_{kin}}{\mu} \tag{18}$$

for any assumed viscosity law, $\mu = \mu(T_{kin})$.

- If N is the number of particles in the cell, calculate

$$N_{coll} = \frac{1}{2}\nu_c N\Delta t \tag{19}$$

collisions, treating all collision pairs as equally likely. If $\nu_c\Delta t > 1$, some particles must undergo more than one collision in the time step.

In the next two sections the results from the new simulation method are compared with the results obtained using DSMC, with standard VHS scattering, and RTSM. In all test

cases I have assumed a viscosity given by

$$\mu = \mu_{ref}\left(\frac{T}{T_{ref}}\right)^{0.81}, \tag{20}$$

which corresponds to $\upsilon = 0.31$. The theoretical viscosities of all models were matched.

5. RELAXATION CALCULATIONS

For five different nonequilibrium distributions of particle velocities in a single 'cell,' simulations were performed to determine the relaxation rates of the different models. The initial conditions are described below. All speeds are expressed in arbitrary units.

1. Half the simulator particles had $v_x = 10$; the remainder had $v_x = -10$. The v_y and v_z components were selected from an equilibrium distribution with a mean of 0 and a most probable thermal speed $(2RT)^{\frac{1}{2}} = 1/10$.
2. As above, expect that v_y, as well as v_x, took values of ± 10.
3. The v_x component of velocity was selected from an equilibrium distribution with a mean of 0 and a most probable thermal speed of $1/100$. The v_y and v_z components were selected from an equilibrium distribution with a mean of 0 and a most probable thermal speed of 10.
4. Each component of velocity was selected from an equilibrium distribution with a mean velocity of 0, but with different kinetic temperatures for each component. The characteristic thermal speeds of the various components were 1, 2, and 4.
5. One fifth of the simulator particles were selected from an equilibrium state with a mean velocity of $(20, 0, 0)$ and a characteristic thermal speed of 3. The remainder were selected from an equilibrium distribution with a mean velocity of 0 and a characteristic thermal speed of 1. This roughly corresponds to a high-speed, high-temperature jet, mixed with a low-temperature gas at rest.

For each initial nonequilibrium distribution the three components of kinetic temperature were different. It was found, as expected, that the difference between any two temperatures decayed with simulated elapsed time. Typical temperature histories from a relaxation simulation are shown in Fig. 1. These curves could be well fit by an equation of the form

$$T_j - T_k = (T_j - T_k)_0 \exp(-\nu_{nom} t/Z),$$

where ν_{nom} is the nominal collision frequency derived from viscosity,

$$\nu_{nom} = \frac{4}{\pi}\frac{\rho R T_e}{\mu} = \frac{4}{\pi}\frac{p_e}{\mu}, \tag{21}$$

where $T_e = (T_x + T_y + T_z)/3$ is the equilibrium temperature. The translational collision number is

$$Z = \nu_{nom} t_c, \tag{22}$$

where t_c is the decay time constant. The data in the range $0.5 < \hat{t} < 2.0$ was used in the curve-fitting to determine Z.

For each of the five initial conditions, three estimates of Z were found, one from each of the three possible pairings $T_x - T_y$, $T_y - T_z$, $T_z - T_x$. The median value of these three

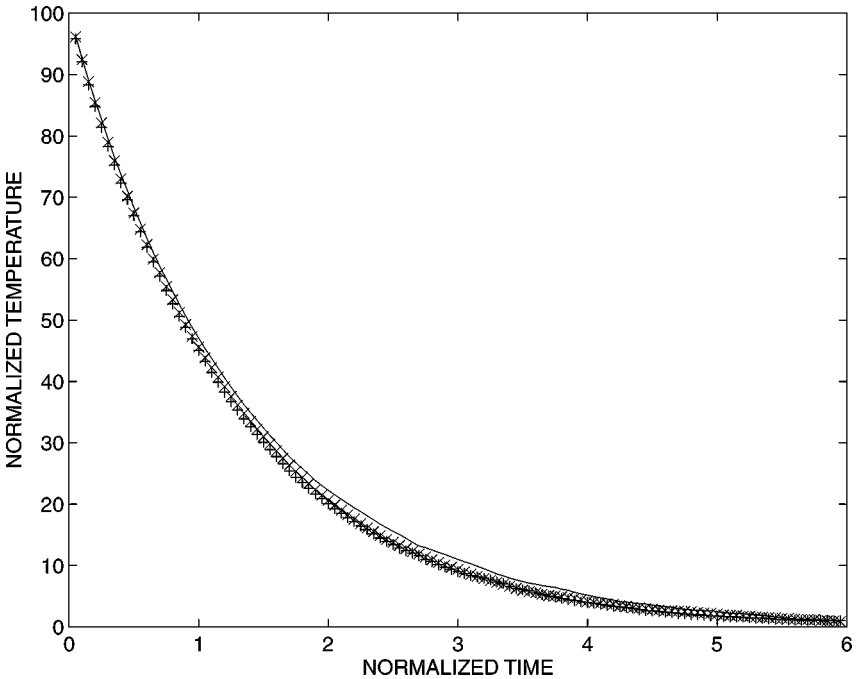

FIG. 1. Typical relaxation history. Temperature difference $\Delta\hat{T} = (T_x - T_y)/T_e$ vs simulation time $\hat{t} = \nu_{nom}t$. Case 1, 80,000 particles: −, DSMC; ×, RTSM; +, ν-DSMC.

estimates was taken as the best estimate of Z. Each simulation was performed for 20,000 simulator particles and was repeated 10 times. The mean and probable error bounds (taken as twice the standard deviation) of the 10 simulations are shown in Table I. For RTSM, the temperature difference should relax with a characteristic time $t_c = \tau$, so the theoretical collision number is

$$Z_{RTSM} = \nu_{nom}\tau = 4/\pi = 1.273\ldots,$$

which is within the error bounds of the data shown in the table.

Both RTSM and ν-DSMC agree with the DSMC calculations, as far as the relaxation rate is concerned; in all cases, the Z values agree within the expected error of two standard deviations. However, this says nothing about the details of the relaxation process. For example, the relaxation time method imposes an equally rapid approach to the equilibrium distribution for all velocity classes, which may not be the case for DSMC and ν-DSMC where new velocities are generated by collisions. Figures 2 and 3 show the thermal speed distribution for case 5, after an elapsed time of one nominal collision interval. It can be seen

TABLE I

Translational Collision Number $Z = \nu_{nom}t_c = 4p_e t_c/(\pi\mu)$

	Case 1	Case 2	Case 3	Case 4	Case 5
DSMC	1.32 ± 0.07	1.32 ± 0.10	1.27 ± 0.14	1.29 ± 0.06	1.23 ± 0.10
RTSM	1.28 ± 0.04	1.29 ± 0.08	1.27 ± 0.08	1.29 ± 0.08	1.28 ± 0.08
ν-DSMC	1.26 ± 0.02	1.28 ± 0.14	1.30 ± 0.18	1.26 ± 0.08	1.27 ± 0.10

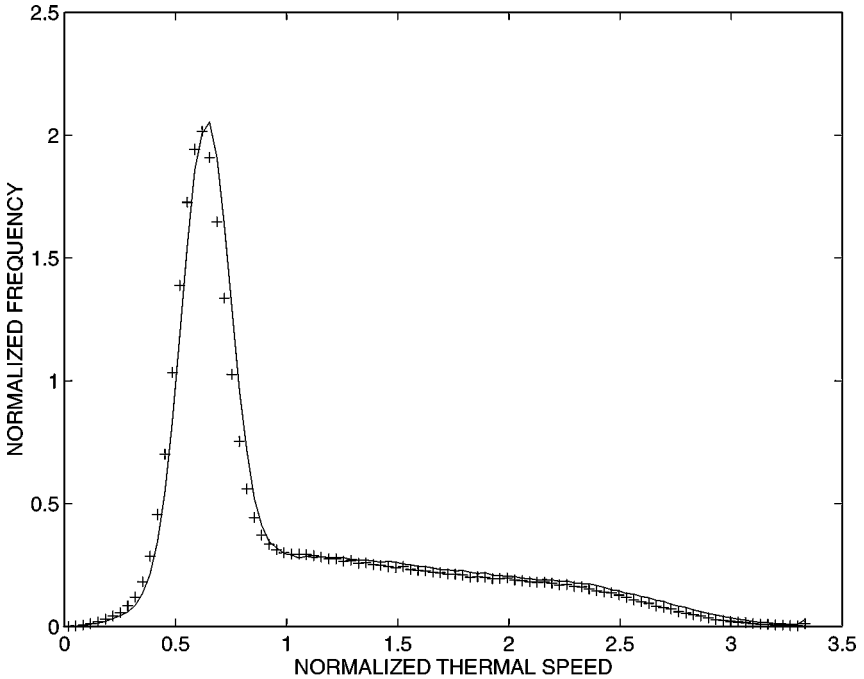

FIG. 2. Thermal speed distribution, $(2RT_e)^{\frac{1}{2}} f$ vs $c(2RT_e)^{-\frac{1}{2}}$, at $t = \nu_{nom}^{-1}$: $+$, ν-DSMC; $-$, DSMC.

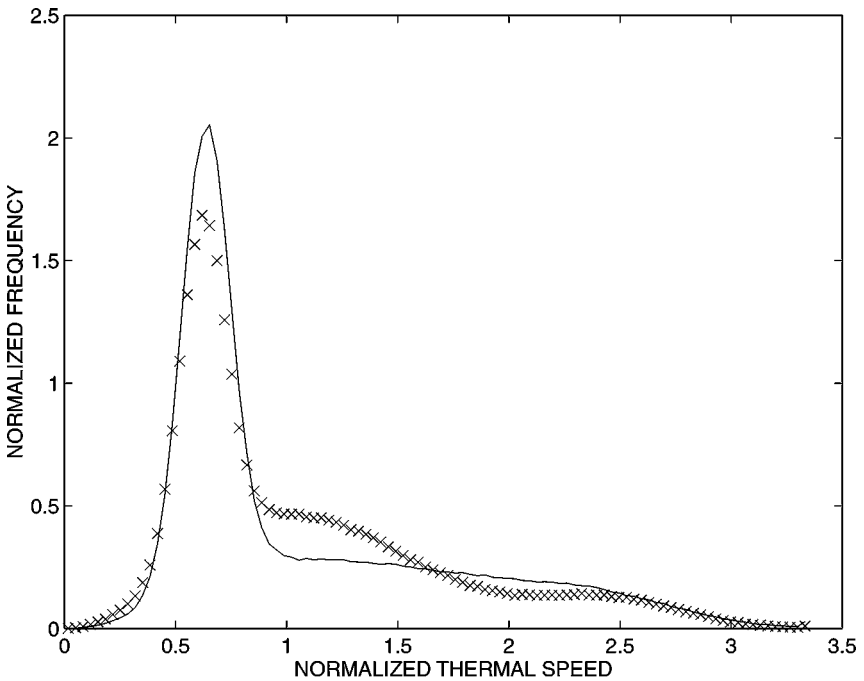

FIG. 3. Thermal speed distribution, $(2RT_e)^{\frac{1}{2}} f$ vs $c(2RT_e)^{-\frac{1}{2}}$, at $t = \nu_{nom}^{-1}$: $\times$, RTSM; $-$, DSMC.

that the relaxation time (BGK) distribution is quite different from that for DSMC, whereas the distribution for ν-DSMC is remarkably similar to that for DSMC.

For DSMC, the collisions are weighted towards greater values of collision speed, so each collision is more effective in driving the distribution function towards equilibrium than are Maxwell–VHS collisions. However, it follows from (16) and (17) that the simulation collision frequency (collisions/simulator particle) for ν-DSMC is

$$\frac{4\Gamma(4-0.31)}{15\Gamma(2-0.31)} \approx 1.21$$

times the simulation collision frequency for DSMC. The effect of the greater number of 'less efficient' collisions of ν-DSMC is similar to the effect of the smaller number of 'more efficient' collisions of DSMC.

Note that new velocities are generated at rates in the ratio $\approx 0.6:1:1.2$ for RTSM, DSMC, and ν-DSMC. Note also that for both RTSM and ν-DSMC every particle velocity has an equal chance of being altered at any stage, whereas for DSMC larger velocities have a greater chance of being altered. Therefore, neither the different simulation collision rate, nor the different distribution of relative velocities in collisions is sufficient to explain the difference between the BGK relaxation time method and ν-DSMC and DSMC; the essential difference appears to be that the new velocity components v_x, v_y, and v_z are correlated when generated by collisions in DSMC and ν-DSMC (and the Boltzmann equation) but are not correlated when generated from the equilibrium distribution in RTSM (and the BGK equation).

The CPU time used by RTSM and ν-DSMC to calculate the number of collisions required to simulate a given elapsed time is less than 10% of that taken by DSMC. The effective speed-up of these approximate methods compared to DSMC, for a given problem, depends on what fraction of the total CPU time is required to calculate the collisions themselves, and what is required for other tasks. For example, in these relaxation calculations, the temperature history was calculated as well as the distribution function, and both RTSM and ν-DSMC required 27–32% of the CPU time required by DSMC.

6. COUETTE FLOW

The second test case was that of one-dimensional Couette flow between two flat plates (both parallel to the x-axis) moving relative to each other with relative speed V_w. The wall temperature was held constant at T_w. The distance between the plates (in the y-direction) was H. An unsteady simulation was performed, with the gas between the plates initially at rest with density ρ_1 and temperature T_1. After an initial flow development time of $t = 10H/(2RT_1)^{\frac{1}{2}}$, successive samples were taken to obtain the time-averaged steady solution.

Only half the flow was simulated. The origin of the y-axis was at the plane of skew symmetry where particles were 'reflected' with x and y velocity components reversed. At the plane $y = H/2$ a diffusely reflecting, moving-wall boundary condition was implemented. The mean x-component of velocity of the diffusely reflected molecules was $V_w/2$.

The flow is completely specified by the nondimensional parameters $T_w/T_1 = 1$ (the wall temperature ratio), $S_w = V_w/(2RT_w)^{\frac{1}{2}} = 2.67$ (the wall speed ratio), and $Kn_1 = \lambda_1/H$ (the Knudsen number), where λ_1 is the nominal mean free path of (6). In all simulations the cell size was $\Delta y < \lambda_1/2$. A fixed time step of $\Delta t = \tau_1/4$ was used, where τ_1 is the relaxation time of (4) evaluated for the initial conditions.

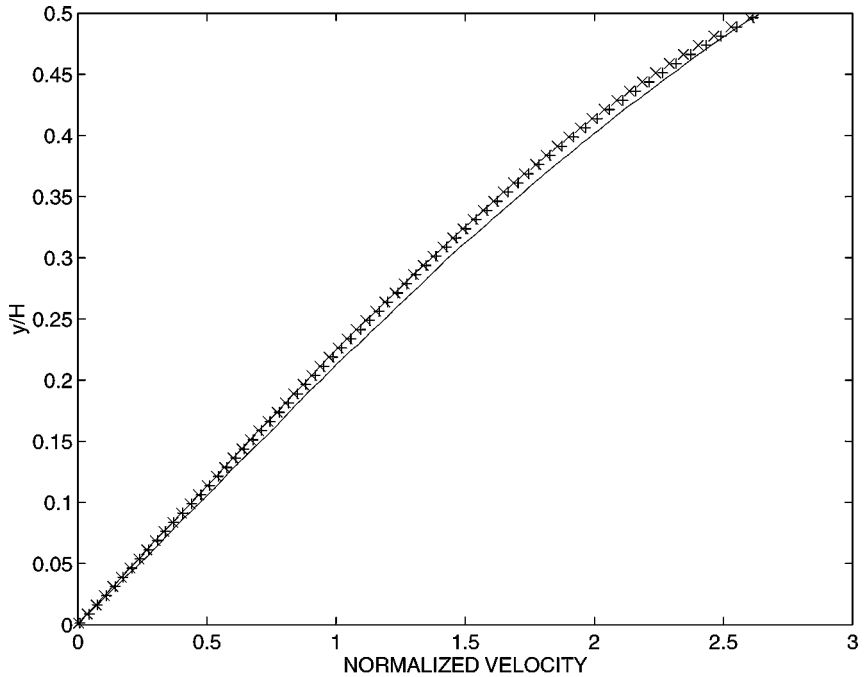

FIG. 4. Couette flow $Kn = 0.005$. Normalized velocity profiles $u_x(\partial RT_w)^{\frac{1}{2}}$ for three simulation methods: $-$, DSMC; $\times$, RTSM; $+$, ν-DSMC. $\tau_1/\Delta t = 4$. 100 cells; $\lambda_1/\Delta y = 2$. For clarity, only 1/3 of points shown.

Figures 4 and 5 show the normalized velocity and temperature profiles for the three simulation methods for the lowest Knudsen number reported here, which is $Kn = 0.005$. The flow velocity (u_x) profiles for all methods are similar. The velocities calculated with ν-DSMC are intermediate between those for DSMC and RTSM. The agreement among the velocity profiles for the three methods was similar for all Knudsen numbers considered. The temperature profile is a sensitive indicator of the differences between the methods. The temperatures for ν-DSMC are within 1% of the DSMC values, while those calculated with RTSM are $\approx$34% greater. Since the work input to the flow is approximately the same for all three models, the rate of heat transfer from the flow to the moving wall should also be the same in the steady state. Since the temperature gradient is greater for RTSM, the coefficient of heat conduction is smaller, as expected from its larger Prandtl number. Figures 6 and 7 show the same effect for Knudsen numbers of $Kn = 0.05$ and $Kn = 0.1$, respectively. The ν-DSMC profiles are very close to those for DSMC, while the RTSM temperature profiles are quite different.

The mean flow temperature for all methods and all Knudsen numbers is shown in Fig. 8. It is mildly surprising that the maximum difference between ν-DSMC and DSMC (5% in the temperature values) occurs for the intermediate Knudsen number of $Kn = 0.05$, rather than for the most rarefied case of $Kn = 0.1$ Also, the difference between the RTSM (BGK) temperature and the DSMC temperature decreases as the Knudsen number increases.

Although they are not shown here, the density profiles for all methods reflect the different temperature profiles; the 'pressure' ρRT was approximately constant to within 3% across the flow for all cases. The mean values of $\rho T/(\rho_1 T_1)$ for DSMC were $\approx$1.60, 1.65, 1.86, and 2.05 for $Kn = 0.005, 0.01, 0.05$, and 0.1, respectively. The ν-DSMC pressure was 0.2% greater than the DSMC pressure for $Kn = 0.005$, and it was 3%, 5%, and 3% less

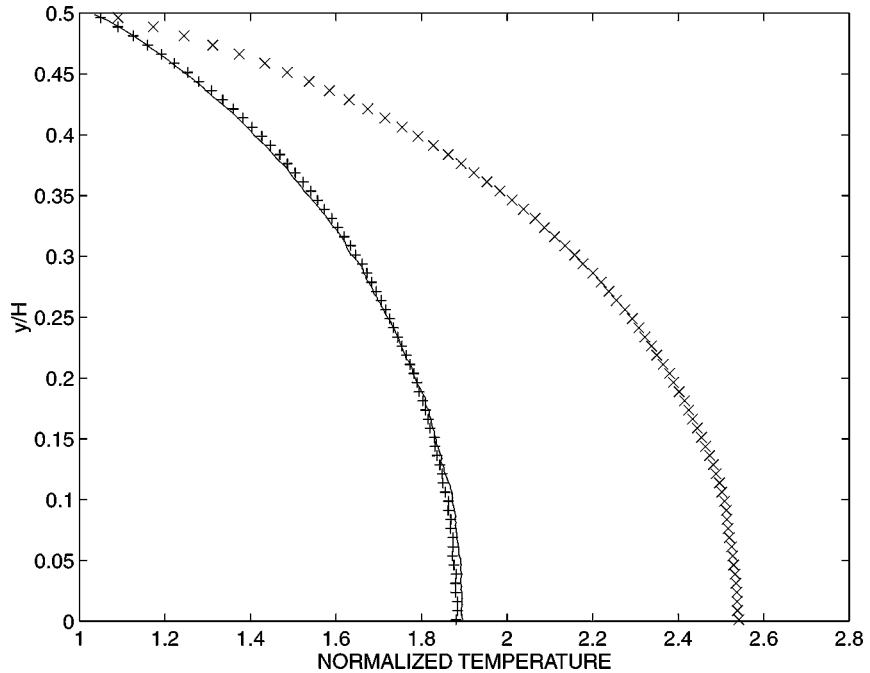

FIG. 5. Couette flow $Kn = 0.005$. Normalized temperature profiles T/T_1 for three simulation methods: $-$, DSMC; $\times$, RTSM; $+$, ν-DSMC. $\tau_1/\Delta t = 4$. 100 cells; $\lambda_1/\Delta y = 2$. For clarity, only 1/3 of points shown. The average ratio of the ν-DSMC temperatures to the DSMC temperatures is 0.99.

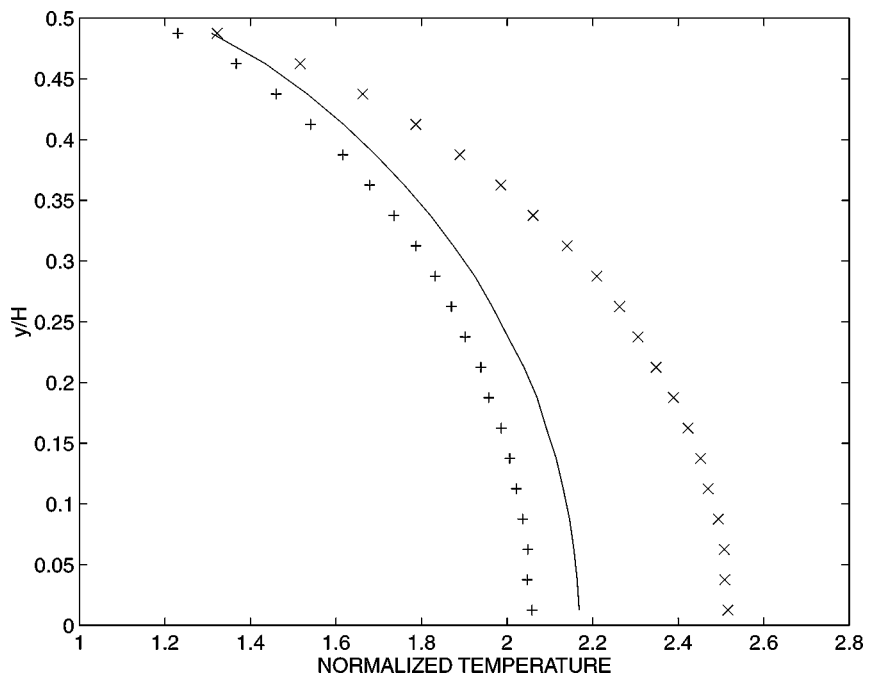

FIG. 6. Couette flow $Kn = 0.05$. Normalized temperature profiles T/T_1 for three simulation methods: $-$, DSMC; $\times$, RTSM; $+$, ν-DSMC. $\tau_1/\Delta t = 4$. 20 cells; $\lambda_1/\Delta y = 2$. The average ratio of the ν-DSMC temperatures to the DSMC temperatures is 0.95 ± 0.01.

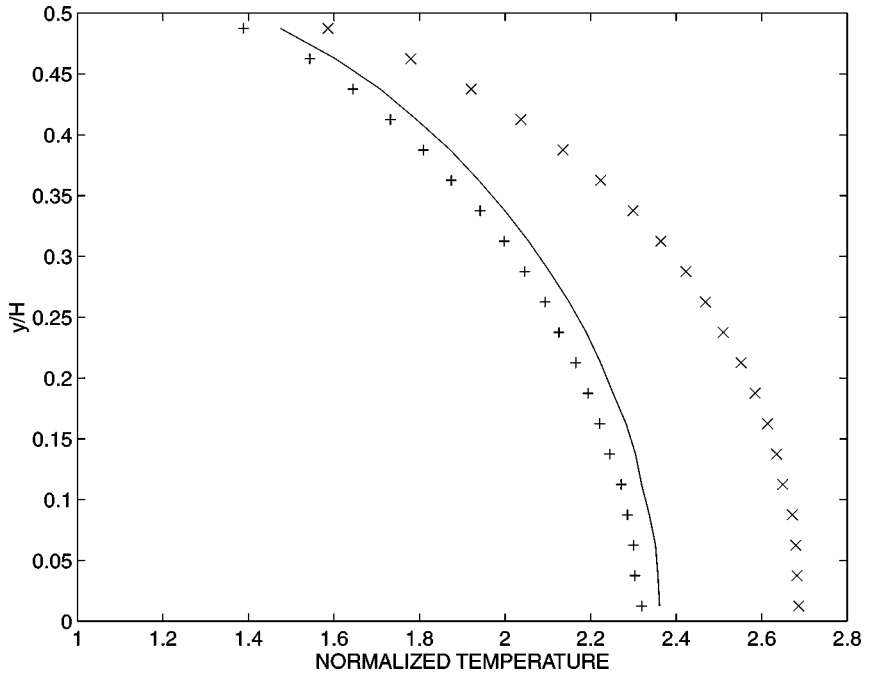

FIG. 7. Couette flow $Kn = 0.1$. Normalized temperature profiles T/T_1 for three simulation methods: −, DSMC; ×, RTSM; +, ν-DSMC. $\tau_1/\Delta t = 4$. 20 cells; $\lambda_1/\Delta y = 4$. The average ratio of the ν-DSMC temperatures to the DSMC temperatures is 0.97 ± 0.02.

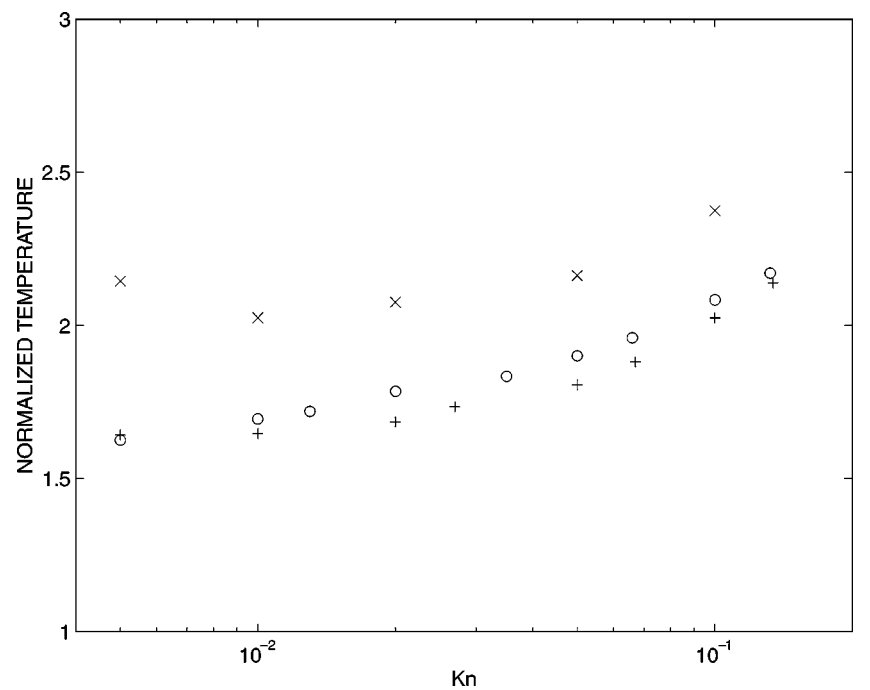

FIG. 8. Mean temperature $(\bar{T}/T_1)$ for Couette flow with $S_w = 5.34$, $T_w/T_1 = 1$: o, DSMC; ×, RTSM; +, ν-DSMC.

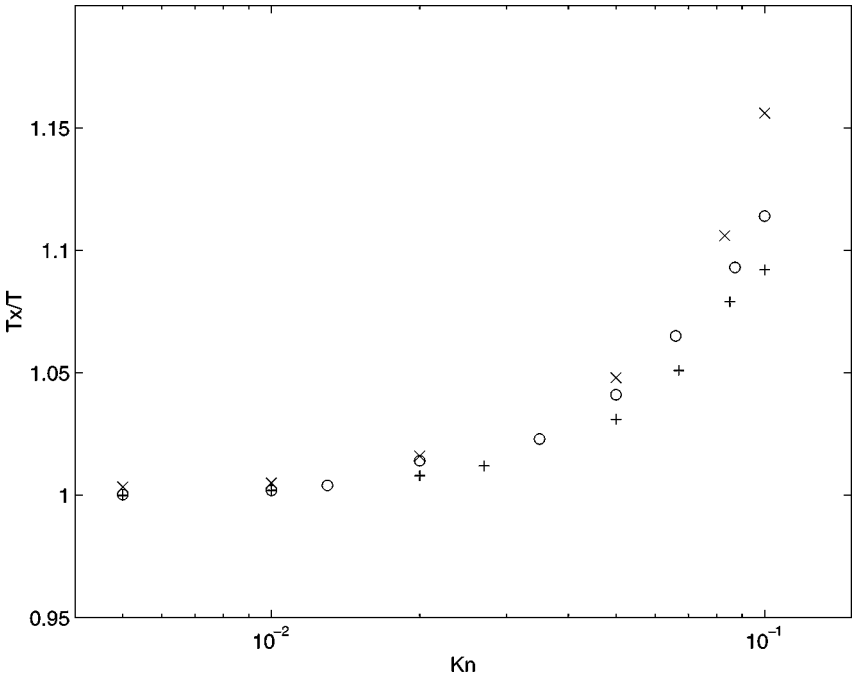

FIG. 9. Approach to equilibrium ($T_x/T \to 1$, mean value for all y) for Couette flow with $S_w = 5.34$, $T_w/T_1 = 1$: o, DSMC; $\times$, RTSM; $+$, ν-DSMC.

for Kn = 0.01, 0.05 and 0.1. For RTSM, the pressures were larger than for DSMC by 28%, 18%, 13%, and 14%, respectively.

Figure 9 shows the approach to equilibrium for the different methods, as measured by the average value of T_x/T, across the flow. As expected $T_x \to T$ as the Knudsen number decreases, for all three methods. The relaxation time method shows a slightly greater departure from equilibrium than do the other two methods.

The velocity distribution functions in the cell closest to the plane of skew symmetry for ν-DSMC and DSMC are compared in Figs. 10 and 11. The figures also show the theoretical equilibrium distribution

$$f_e = (2\pi RT_x)^{-\frac{1}{2}} \exp\left[-c_x^2/(2RT_x)\right],$$

where $c_x = v_x - \bar{v}_x$ is the x-component of thermal velocity and T_x is the x-component of kinetic temperature (from the DSMC results). The DSMC results are very close to this theoretical distribution for $Kn = 0.01$, but a small departure from equilibrium can be seen for $Kn = 0.1$. It is clear that the DSMC and ν-DSMC results agree very closely for both the low $Kn = 0.01$ and high $Kn = 0.1$ Knudsen numbers. At $Kn = 0.005$, the distributions for DSMC and ν-DSMC (not shown) are virtually indistinguishable.

7. THE PLANE NORMAL SHOCK

As a final test case, the structure of a plane shock has been calculated by DSMC, ν-DSMC, and RTSM. The upstream Mach number is $M_1 = 8$ and, as in all calculations presented here, the theoretical viscosity varied as $T^{0.81}$. The conditions correspond to the test case, 'strong

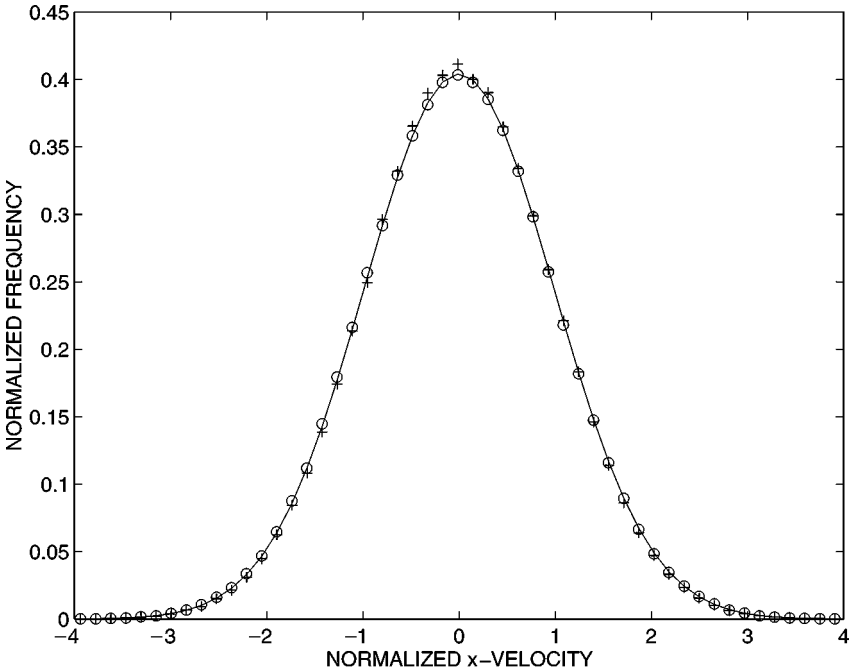

FIG. 10. Distribution of x-component of thermal velocity, $(2RT_1)^{\frac{1}{2}} f$ vs $c_x(2RT_1)^{-\frac{1}{2}}$, where $c_x = v_x - \overline{v}_x$ and $f(c_x)$ is the thermal velocity distribution function. $Kn = 0.01$ and $y/H = 2.5 \times 10^{-3}$. The solid line is the theoretical distribution for equilibrium at temperature $T_x/T_1 = 1.953$ (DSMC value). o, DSMC; +, v-DSMC.

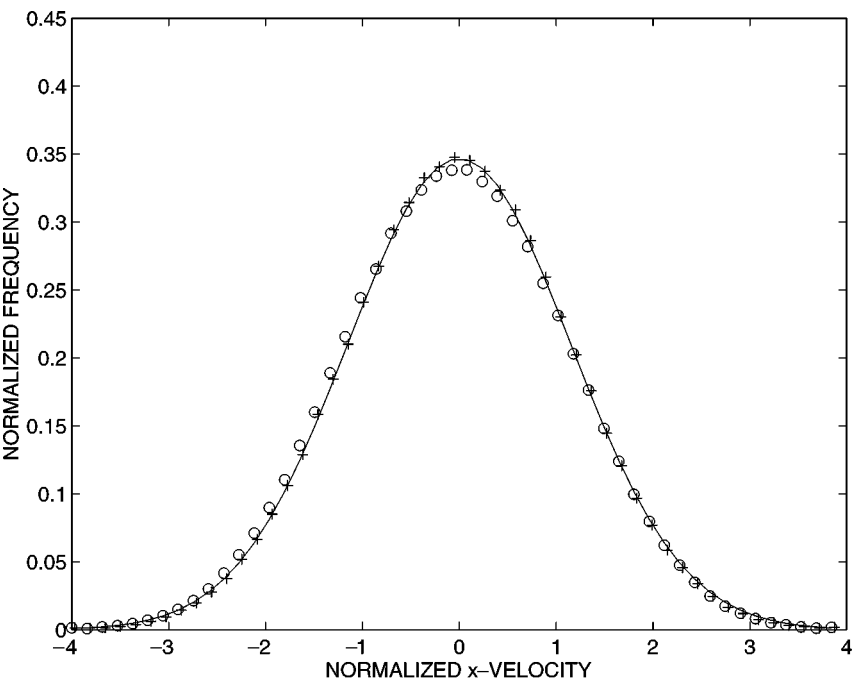

FIG. 11. Distribution of x-component of thermal velocity, $(2RT_1)^{\frac{1}{2}} f$ vs $c_x(2RT_1)^{-\frac{1}{2}}$, where $c_x = v_x - \overline{v}_x$ and $f(c_x)$ is the thermal velocity distribution function. $Kn = 0.1$ and $y/H = 1.25 \times 10^{-2}$. The solid line is the theoretical distribution for equilibrium at temperature $T_x/T_1 = 2.643$ (DSMC value). o, DSMC; +, v-DSMC.

shock in argon,' presented by Bird [3]. A shock was produced in the shock-stationary frame of reference, and Bird's [3] stability procedure was used to counteract the possible smearing of the shock profiles arising from the slow random walk variation of the shock location. That is, the cell network was shifted slightly upstream or downstream throughout the simulation, to keep the total number of particles in the simulation approximately constant.

The initial conditions (upstream ρ_1, T_1, V_1 and downstream ρ_2, T_2, V_2) were set from the Rankine–Hugoniot conditions, with a discontinuity between upstream and downstream conditions at $x = 0$. The initial flow region extended over a distance $-x_1 < x < x_2$. At each time step, before the particles were moved, new upstream particles were created, uniformly distributed in position over the region $-x_1 - V_{max}\Delta t < x < -x_1$, where $V_{max} = V_1 + 3(2RT_1)^{\frac{1}{2}}$ was the 'cut-off' speed of any particle entering the flow from upstream. The number density of these new particles was $n_1 = \rho_1/m$, and their velocities were selected from an equilibrium distribution with a mean of V_1 and a variance of RT_1. While the particles were moved, those downstream could interact with a specularly reflecting surface, initially at $x = x_2$ and moving with the theoretical downstream flow speed V_2. Before the start of the next time step, the origin of the x-coordinate of all particles was moved a distance $V_1\Delta t$ upstream, and then all particles with position outside the range $-x_1 \le x \le x_2$ were deleted. While the implementation of the downstream condition is the same as that used previously [3, 9], the upstream implementation is slightly different from usual. Time-averaged samples were taken after an elapsed simulation time of $5(x_1 + x_2)/V_1$. The cell size was $\Delta x = 0.85\lambda_2$, where $\lambda_2 = 2\mu_2/(\rho_2\bar{c}_2)$ is the nominal mean free path behind the shock. The decoupling interval was $\Delta t = 0.9\lambda_2/\bar{c}_2$.

Figure 12 shows the normalized density and temperature profiles for DSMC, ν-DSMC, and the RTSM solution of the BGK equation. For clarity, only every second point in the

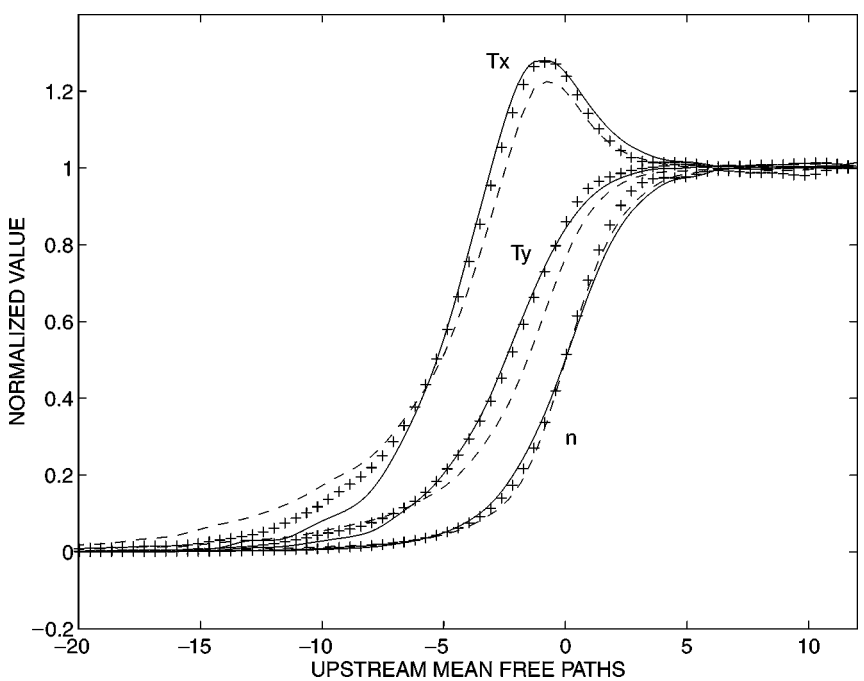

FIG. 12. Density $\hat{n} = (n - n_2)/(n_2 - n_1)$ and temperature $\hat{T}_j = (T_j - T_{j,1})/(T_{j,2} - T_{j,1})$ vs x/λ_1 in a normal shock. $M = 8$, $\gamma = 5/3$, $\mu = \mu_1(T/T_1)^{0.81}$: $-$, DSMC; $+$, ν-DSMC (every second point omitted for clarity); $--$, RTSM (BGK equation).

ν-DSMC results is shown. The origin of the x-axis for each set of results has been set at the point where $n = (n_1 + n_2)/2$. Both ν-DSMC and RTSM results differ from the DSMC results, but the ν-DSMC results are significantly better than those for RTSM. The location and magnitude of the peak T_x is well represented by ν-DSMC, as is the location of the T_y profile; there is a slightly longer upstream precursor than DSMC for both T_x and T_y and a slightly shorter downstream tail. The overall agreement, however, is good and better than the agreement between DSMC and the BGK solution from RTSM. The average deviation of the ν-DSMC values from the DSMC values, over the interior of the shock (taken as $-10\lambda_1 < x < 5\lambda_1$), is 1.7% of the downstream value for density, 2.8% for T_x, and 1.4% for T_y, which is consistent with the error of $\approx$5% found in the relaxation and Couette flow test cases. The corresponding values for the RTSM solution of the BGK equation are 1.7%, 6.0%, and 4.8%.

8. COMPUTATIONAL EFFORT

To calculate collisions only, ν-DSMC requires about 10% of the computational effort of DSMC. The total computational effort for ν-DSMC compared to DSMC depends on what fraction of the total CPU time is consumed by the collision calculations. For very small time steps $\Delta t/\tau \ll 1$, very few particles undergo a collision in any time step and the overhead of establishing the list of collision partners and calculating the kinetic temperature is significant. For the Couette flow, with $\Delta t/\tau = 0.25$, ν-DSMC required almost 80% of the CPU time required for DSMC. Larger values of Δt are often used (in an effort to reduce the computational load), and in that case ν-DSMC becomes relatively better. For example, for the Couette flow, with $\Delta/\tau = 0.50$, the CPU requirements dropped to 50% of that required for DSMC. For the plane shock case, the ratio of $\Delta t/\tau$ was 0.9 downstream of the shock, but 0.13 upstream, and ν-DSMC required 60% of the CPU required by DSMC. The codes were written in the Matlab programming language.

9. CONCLUSION

ν-DSMC is a new approximate simulation method for rarefied flows which takes advantage of the simplified collision probability of a Maxwell total collision cross-section, modified by making the total collision cross-section a function of kinetic temperature. More collisions are calculated for ν-DSMC than for DSMC and, in this way, the theoretical viscosity of each method is equal for near-equilibrium conditions. Any variation of viscosity with temperature, $\mu = \mu(T)$, can be achieved with ν-DSMC. Because collision pairs can be selected independently of the collision velocity, the collision calculations require less computational effort.

It is natural to inquire if the new method, which was constructed from equilibrium or near-equilibrium assumptions, works well in highly nonequilibrium conditions. Here the test must be whether the new method produces results which are close to those produced by DSMC. The collision phase of *any* DSMC calculation consists of a zero-dimensional relaxation calculation in every cell at every time step. If it could be shown that a method produced the same velocity distribution as DSMC after any simulated relaxation time, for any initial velocity distribution, the method would then necessarily produce the same results as DSMC for any simulated flow. Hence the first test undertaken here was to compare the

distribution of molecular speeds with that produced by DSMC for a number of different initial velocity distributions, which were examples of extreme nonequilibrium conditions. ν-DSMC produced a speed distribution remarkably similar to that produced by DSMC after one mean collision time, whereas the solution of the BGK equation gave a very different distribution, despite all methods giving the same relaxation rates for the kinetic temperatures.

The remaining test cases were designed to investigate the extent to which differences in the relaxation process affected the flow properties in two realistic non-equilibrium flow situations, high speed Couette (shear) flow and the interior of a strong shock. The results were as might be expected from the relaxation tests, and from the theoretical knowledge that the BGK equation predicts a Prandtl number of 1, rather than the correct value of $2/3$. It was found that the new method agreed with DSMC to within about 5% or less, while the agreement for the RTSM solution of the BGK equation was no better than 10 or 15% in most cases.

If an approximate method for rarefied flow is deemed sufficient, or necessary because of CPU limitations, it is clearly better to use ν-DSMC, rather than settle for a solution of the BGK equation. The approximate simulation provided by ν-DSMC requires computational effort similar to that required to solve the BGK equation and yields superior results. Most important is the fact that the Prandtl number is correct for the approximate method but not for the solution of the BGK equation.

APPENDIX: SOME PROGRAMMING DETAILS

1. The collision pairs are preselected to facilitate parallel computation. Here I assume that $1 < \nu_c \Delta t < 2$ so that more than one collision is required for some particles. Collisions are calculated in stages so that no particle undergoes more than one collision at any stage. The particles in the cell are arranged in a list, numbered $j = 1, 2, \ldots N$. In one-dimensional flows, adjacent particles in this list can be nearest neighbours, while for two- and three-dimensional flows adjacent particles in this list can be near, if not necessarily nearest, neighbours.

First collisions: The collision pairs are arranged as follows:

particle number	1	3	5	7	...
collides with	|	|	|	|	
particle number	2	4	6	8	....

In this stage each particle undergoes one collision, which corresponds to an elapsed time of $\nu_c \Delta t = 1$. If $\nu_c \Delta t < 1$, not every collision pair from the above list need undergo a collision and no second stage is required. In that case, collisions are calculated between pairs starting from a randomly chosen initial position in the list.

Second collisions: The collision pairs are arranged as follows:

particle number	1	3	5	7	...
may collide with	|	|	|	|	
particle number	4	2	8	6	....

Collisions are calculated between pairs starting from a randomly chosen initial position in this list. Note that for accuracy of the decoupling assumption, Δt should be less than τ_{nom}

from (7) (i.e., $\nu_c \Delta t < \pi/2$) so that two stages is all that is usually required. If $\nu_c \Delta t > 2$ (as may be allowed in some near-continuum calculations), the above procedure can be extended to an arbitrary number of stages. However, in that case, after two or three collisions/particle have been calculated, it might be just as good to use the relaxation time method to account for the remaining collisions.

2. Following Bird [3], I have used the time-averaged number of particles in each cell, $\bar{N}$, when calculating the number density in (18) which determines the collision rate. The time-averaged value is used to reduce statistical scatter in steady state solutions but it can have the effect of introducing errors in the unsteady development of the flow. I have calculated the time average using a decreasing weight on previous values. Let $\bar{N}_{j-1}$ be the time-averaged valued up to time step $j-1$. At time step j, the past samples which went into calculating $\bar{N}$ are multiplied by a weighting factor w, where $w < 1$. Thus

$$s_j = w s_{j-1} + 1 \tag{A.1}$$

$$\bar{N}_j = (N(j) + w \bar{N}_{j-1})/s_j. \tag{A.2}$$

I have used $w = 0.95$ in the work reported here.

3. The particles in any cell represent the much larger number of particles at that location in the real gas and can be thought of as a sample selected from the true parent distribution. The temperature of the parent distribution is related to the variance of each component of velocity:

$$T = (T_x + T_y + T_z)/3$$

$$T_{k=x,y,z} = \sum_{j=1}^{N} (v_{k,j} - \bar{v}_k)^2/(NR)$$

$$\bar{v}_{k=x,y,z} = \sum_{j=1}^{N} v_{k,j}/N.$$

It is a standard result of statistical theory that the best estimate of the parent variance is

$$s^2 = \sum_{j=1}^{N} (x_j - \bar{x})^2/(N-1),$$

where s is the sample standard deviation. Following Roveda *et al.* [16], I have estimated the kinetic temperature in a cell from the sample variance as

$$T_{k=x,y,z} = \sum_{j=1}^{N} (v_{k,j} - \bar{v}_k)^2/((N-1)R). \tag{A.3}$$

ACKNOWLEDGMENT

The Australian Research Council supported this work under Grant 97/ARCL99.

REFERENCES

1. P. L. Bhatnagar, E. P. Gross, and M. Krook, Model for collision processes in gases, I, *Phys. Rev.* **94**, 511 (1954).

2. G. A. Bird, Monte-Carlo simulation in an engineering context, in *Rarefied Gas Dynamics: Proceedings of the 12th International Symposium, New York*, edited by S. Fisher (AIAA Press, Washington, DC, 1981).
3. G. A. Bird, *Molecular Gas Dynamics and the Direct Simulation of Gas Flow* (Clarendon, Oxford, 1994).
4. C. Borgnakke and P. S. Larsen, *Statistical Collision Model for Monte–Carlo Simulation of Polyatomic Gas*, Technical Report AFM 73-08, Dept. Fluid Mechanics, Technical Univ. of Denmark, Lyngby (1973).
5. C. Borgnakke and P. S. Larsen, Statistical collision model for Monte–Carlo simulation of polyatomic gas mixture, *J. Comput. Phys.* **18**, 405 (1975).
6. S. Chapman and T. G. Cowling, *The Mathematical Theory of Nonuniform Gases*, 3rd ed. (CUP, Cambridge, UK, 1970).
7. A. I. Erofeev and V. A. Perepukhov, Hypersonic rarefied flow about a flat plate by the Direct Simulation Method, in *Rarefied Gas Dynamics: Proceedings of the 11th International Symposium*, edited by R. Campague (Centre d'Etudes Scientifiques et Techniques d'Aquitane CEA/CESTA, Paris, 1979), p. 417.
8. P. I. Larsen and C. Borgnakke, Statistical collision model for simulating polyatomic gas with restricted energy exchange, in *Rarefied Gas Dynamics: Proceedings of the 19th International Symposium, Porz-Wahn, Germany*, edited by M. Becker and M. Fiebig (DFVLR, 1974).
9. M. N. Macrossan, *Diatomic Collision Models used in the Monte–Carlo Direct Simulation Method Applied to Rarefied Hypersonic Flows*, Ph.D. thesis (The University of London, 1983).
10. M. N. Macrossan, A particle simulation method for the BGK equation, in *Rarefied Gas Dynamics: Proceedings of the 22nd International Symposium, Sydney, 2000*, edited by T. Bartel and M. Gallis (Am. Inst. of Phys., New York, 2001), Ch. 6.10.
11. J. M. Montanero, J. W. Duffy, and J. F. Lutsko, Stability of uniform shear flow, *Phys. Rev. E* **57**, 547 (1998).
12. K. Nanbu, Direct simulation scheme derived from the Boltzmann equation. I. Monocomponent gases, *J. Phys. Soc. Jpn.* **49**, 2042 (1980).
13. K. Nanbu, On the simulation of the Bhatnagar–Gross–Krook equation, *J. Phys. Soc. Jpn.* **50**(9), 3154 (1981).
14. K. Nanbu, S. Igarashi, and Y. Watanabe, Stochastic solution method of the model kinetic equation for a diatomic gas, *J. Phys. Soc. Jpn.* **57**(10), 3371 (1988).
15. D. I. Pullin, Direct simulation methods for compressible ideal gas flow, *J. Comput. Phys.* **34**, 231 (1980).
16. R. Roveda, D. B. Goldstein, and P. L. Varghese, Hybrid Euler/particle approach for continuum/rarefied flows, *J. Spacecraft Rockets* **35**(3), 258 (1998).